The Mechanism of Stress Corrosion Cracking in Sensitized Austenitic Stainless Steels in Nuclear Power Reactor Heat Transport Circuits

Digby D. Macdonald and Jiangbo Shi
Department of Nuclear Engineering
University of California at Berkeley
Berkeley, CA, USA.
macdonald@berkeley.edu

Presented at

SUSTECH 2014

Portland, OR

July 24 – 26, 2014

Outline

- Experimental determination of the electrochemical/mechanical character
- Development of an Artificial Neural Network (ANN) to establish relationships between the dependent variable (crack growth rate, CGR) and the independent variables (K_I, ECP, conductivity, temperature, pH, degree of sensitization, flow velocity).
- Determination of the relative impact of each independent variable on the dependent variable, in order to determine the "character" of IGSCC.
- A viable physico-electrochemical, deterministic/mechanistic model should reflect that same character, since it must be based upon a general empitical model.
- One candidate model is the Coupled Environment Fracture Model (CEFM), which is a mechanico-electrochemical model previously developed by Macdonald and co-workers to predict CGR in sensitized Type 304SS in BWR primary coolant environments.
- Summary of the findings and the conclusions drawn therefrom.

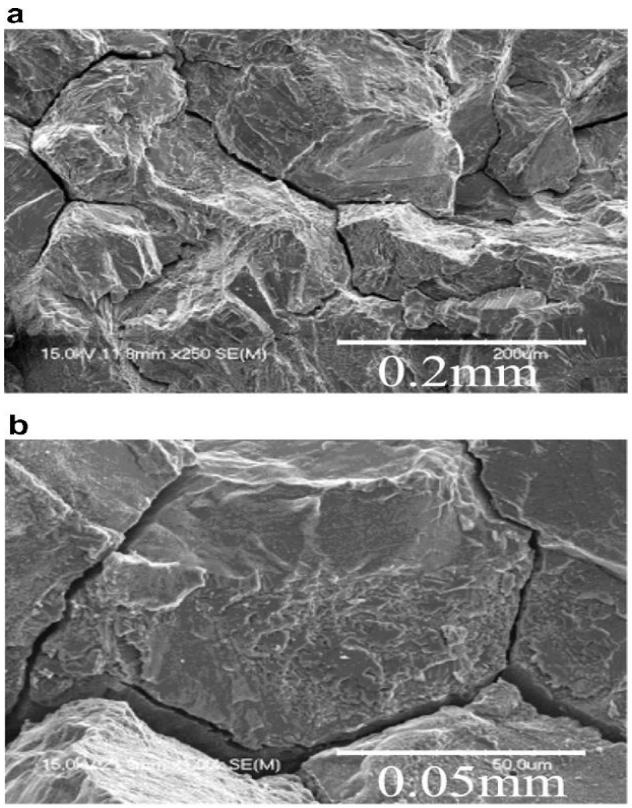

The SEM morphologies of the fracture surface of the 316L weld HAZ specimen after SCC test. (a) In-situ precracking and SCC areas, (b) one typical SCC area.

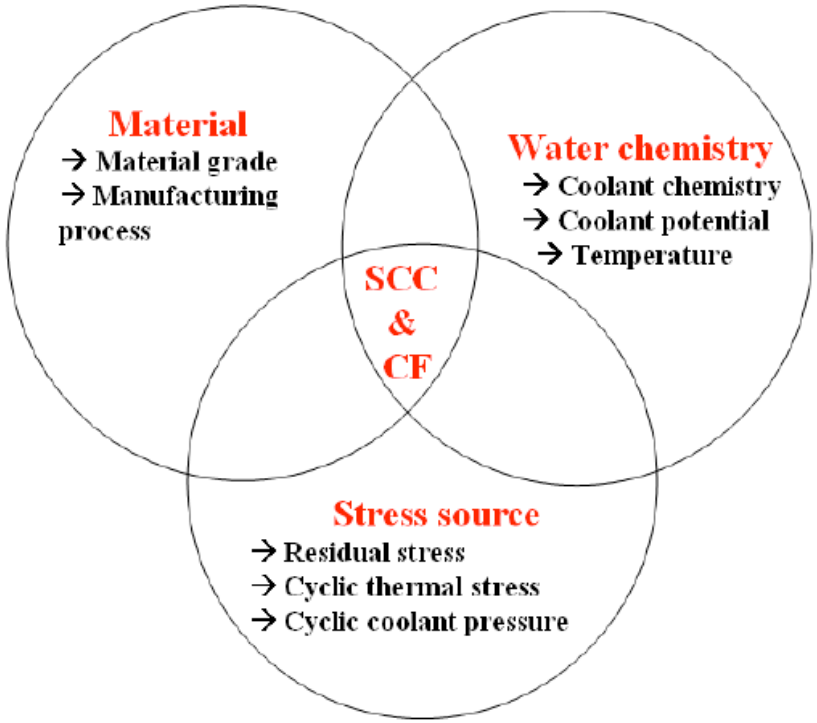

Interaction of parameters in affecting IGSCC in stainless steels in reactor coolant.

The Experimental Facts

- **Localized corrosion, including IGSCC in sensitized stainless steels, generally follows the differential aeration hypothesis (Evans, 1927).**
- **A positive "coupling current" flows through the solution from the crack mouth to the external surfaces, while an equal but opposite electron current flows through the metal in the reverse direction (Figure 1). The two currents annihilate quantitatively via a charge transfer reaction (reduction of oxygen and or hydrogen evolution).**
- **The crack growth rate increases roughly exponentially with the potential of the metal at sufficiently high potentials. At lower potentials, the CGR is potential-independent, corresponding to mechanical creep (Figure 3).**
- **The CGR depends upon the magnitude of the electrochemical crack length, which is defined as being the shortest distance between the crack front and the exposed external surface. This length is generally different from the mechanical loading crack length.**
- **The CGR increases with the DOS and extent of cold work in a sigmoidal fashion.**
- **The environmentally-mediated CGR is proportional to the magnitude of the coupling current.**
- **Coating the external surfaces with an insulator, and hence inhibiting the reduction of oxygen, causes the coupling current to sharply decrease and the crack to stop growing.**
- **Catalyzing the reduction of oxygen on the external surface results in an increase in the coupling current and hence an increase in the CGR.**
- **The crack growth rate is a positive function of the solution conductivity (i.e., the CGR increases with increasing conductivity).**
- **Enhanced mass transfer of oxygen to the external surfaces increase the CGR. For a sufficiently, short, open crack increasing flow rate may destroy the aggressive conditions that develop within the cavity and hence inhibit crack growth.**
- **CGR vs temperature passes through a maximum at 100^{o}C to 200^{o}C.**

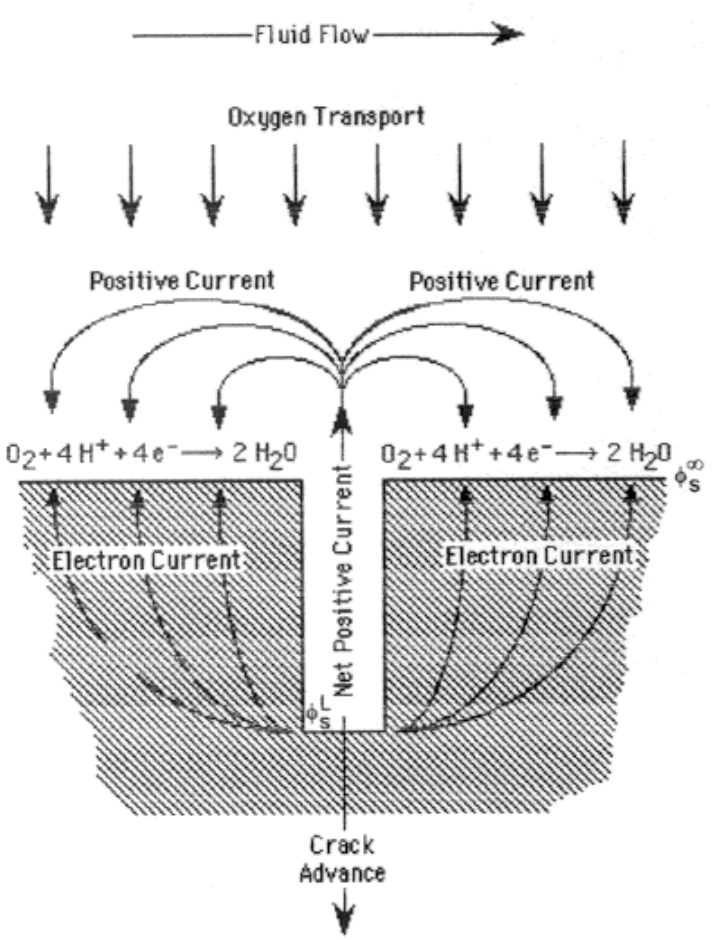

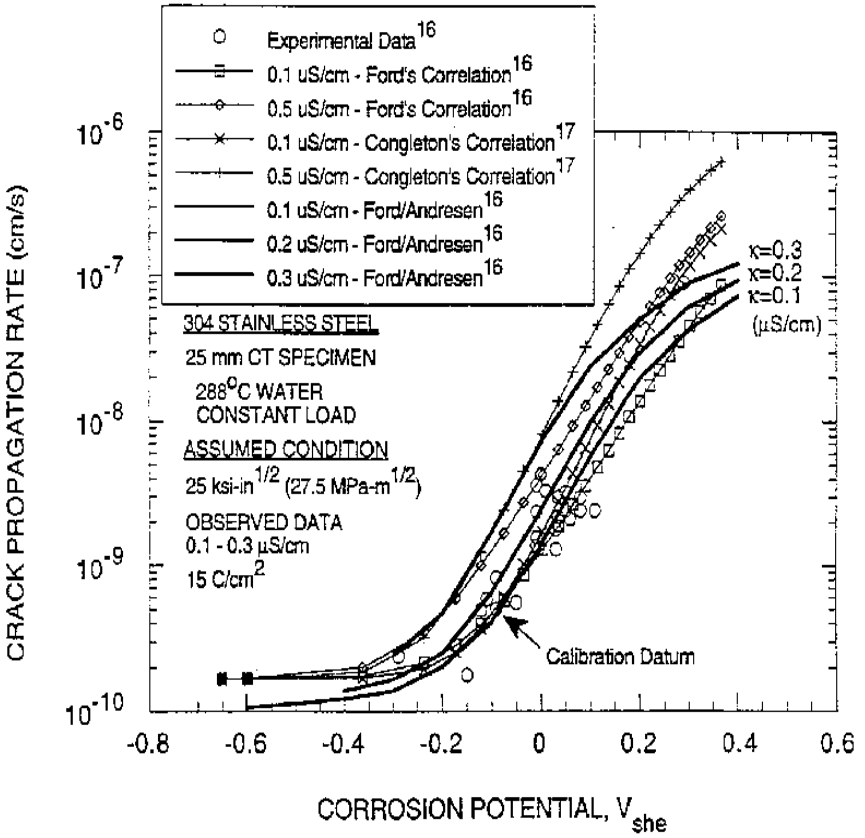

Schematic of the origin of the coupling current in stress corrosion cracking. The differential aeration hypothesis for localized corrosion, and the conservation of charge requires that the electron current flowing from the crack to the external surface must be equal to the positive ionic current flowing through the solution from the crack to the external surface.

Measured and calculated (via the CEFM) crack growth rates for sensitized Type 304 SS in high temperature aqueous solutions as a function of ECP and conductivity. The citations refer to references in the original source [2].

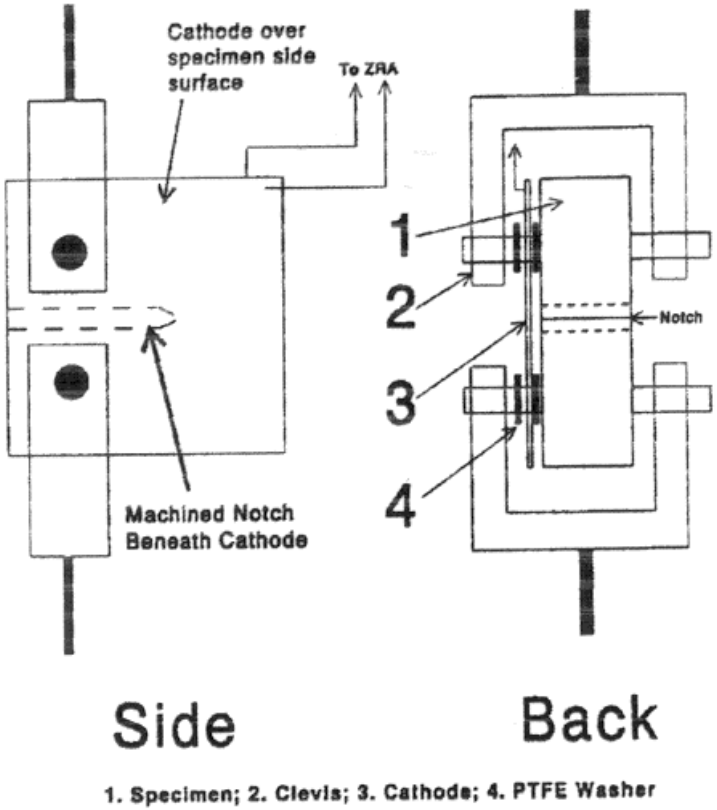

1. Specimen; 2. Clevis; 3. Cathode; 4. PTFE Washer

Specimen configuration used in detecting and measuring the coupling current flowing from a crack to the external metal surface. Note that the C (T) fracture mechanics specimen is coated with PTFE to inhibit the cathodic reduction of oxygen on the specimen surface. Instead, the current flows from the crack to the side cathodes (only one shown) where it is consumed by O_2 reduction. The electron current flows from the crack tip to the side cathodes via a zero resistance ammeter, which is used for its measurement.

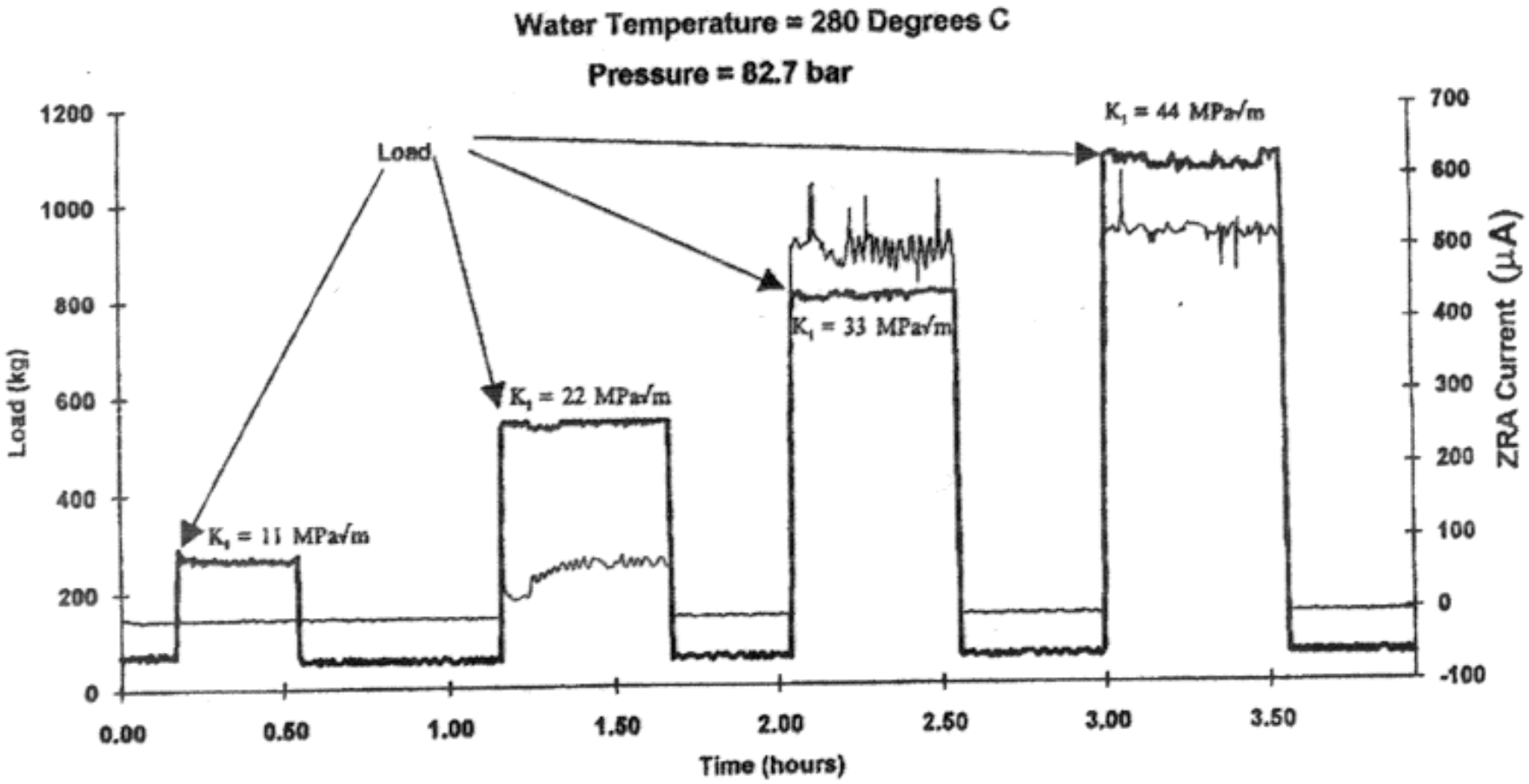

Coupling current and stress intensity versus time for Type 304 SS in simulated BWR coolant at 288 ^{o}C. The specimen was equipped with one platinized nickel side cathode [9].

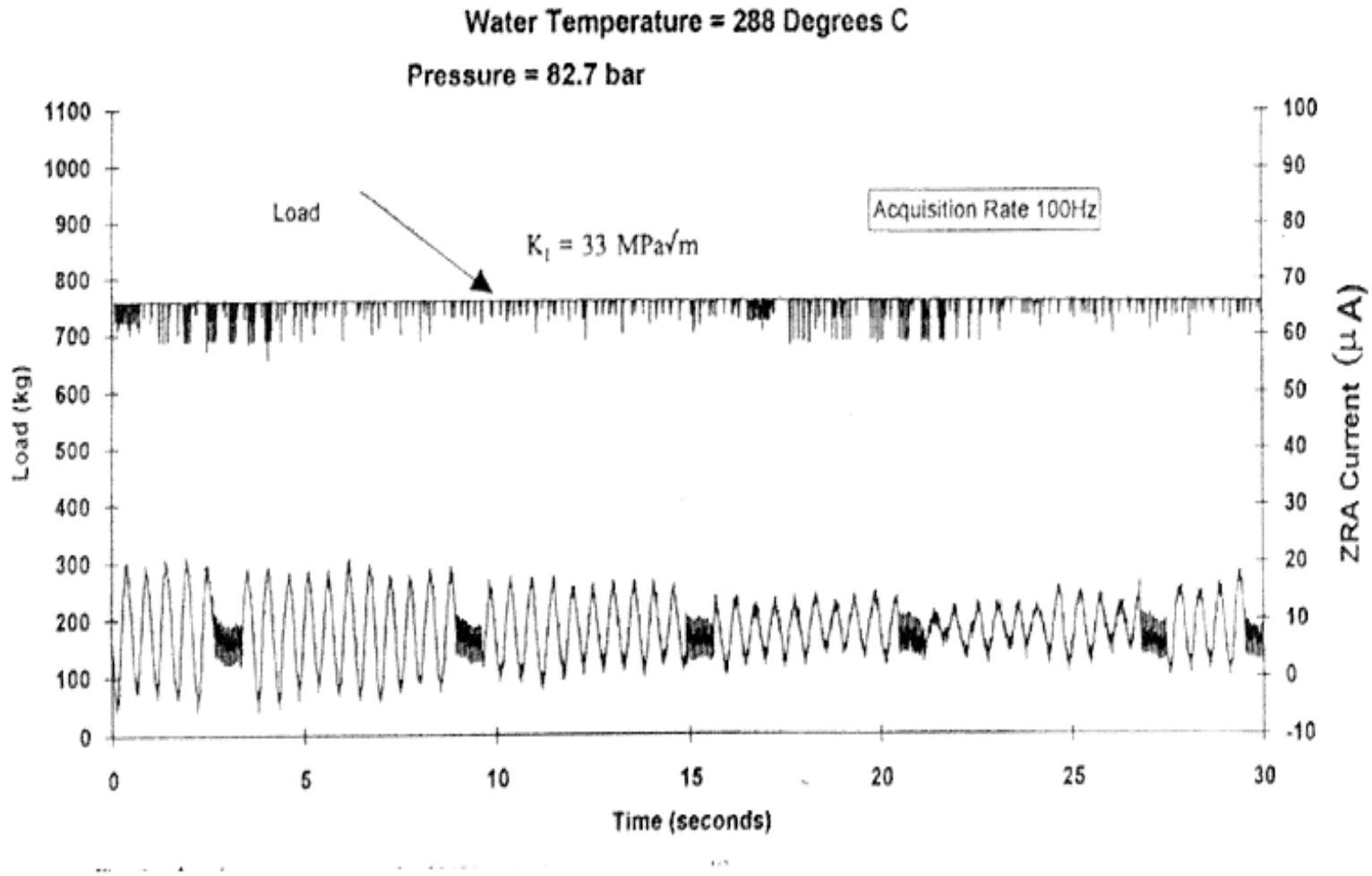

Typical form of the noise in the coupling current for Type 304 SS with two Type 304 SS side cathodes in simulated BWR coolant at 288°C and at a stress intensity of 27.5 MPa√m [9].

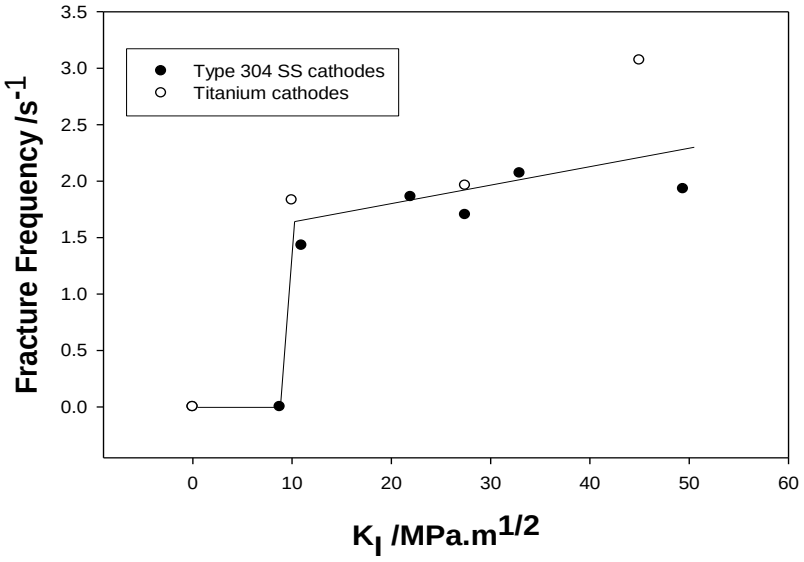

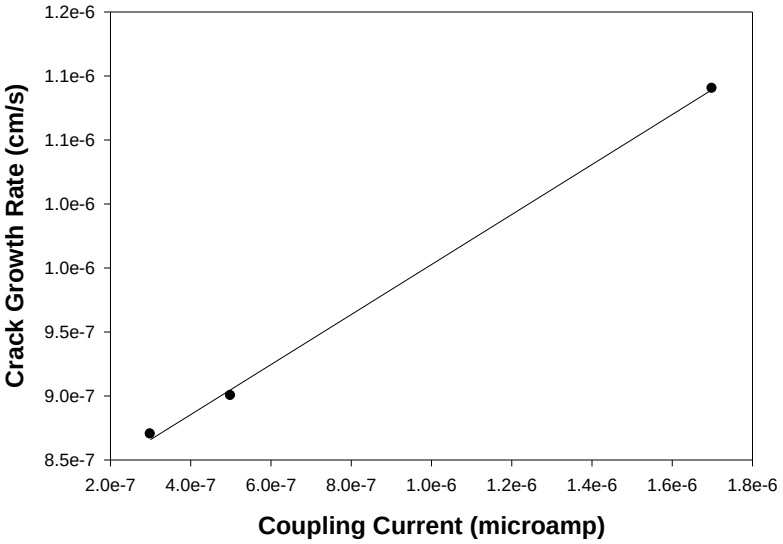

Frequency of the brittle micro fracture events versus stress intensity factor for IGSCC in sensitized Type 304 SS in water at 288 ^{o}C, κ (25 ^{o}C) = 0.5-1.3 μS/cm, [O_2] = 0.15 x 10^{-3} m [9].

Relationship between the crack growth rate and coupling current for IGSCC in sensitized Type 304 SS in oxygenated (7.6 ppm, 2.38 x 10-4 m) sodium chloride (50 ppm, 8.62 x 10-4 m) solution at 250 ^{o}C.

Table 1. Fracture parameters for IGSCC in sensitized Type 304 SS in simulated BWR environments (288 ^{o}C), in 0.5 M thiosulfate solution at ambient temperature (22 ^{o}C), and in AISI 4340 steel in 6 M NaOH at 70 ^{o}C.

System	dL/dt (cm/s)	f (s^{-1})	W/B(cm)	a / μm
304SS/BWR coolant, 288^{o}C [9].	0.78×10^{-7}	2	1.27/1.91	1.93
304SS/Thiosulfate, 25^{o}C [11].	1.70×10^{-6}	0.1 to 0.01	1.416/2.12	42-134
AISI 4340/6m NaOH, 70^{o}C [10].	5.30×10^{-8}	0.003	2.70/4.05	60

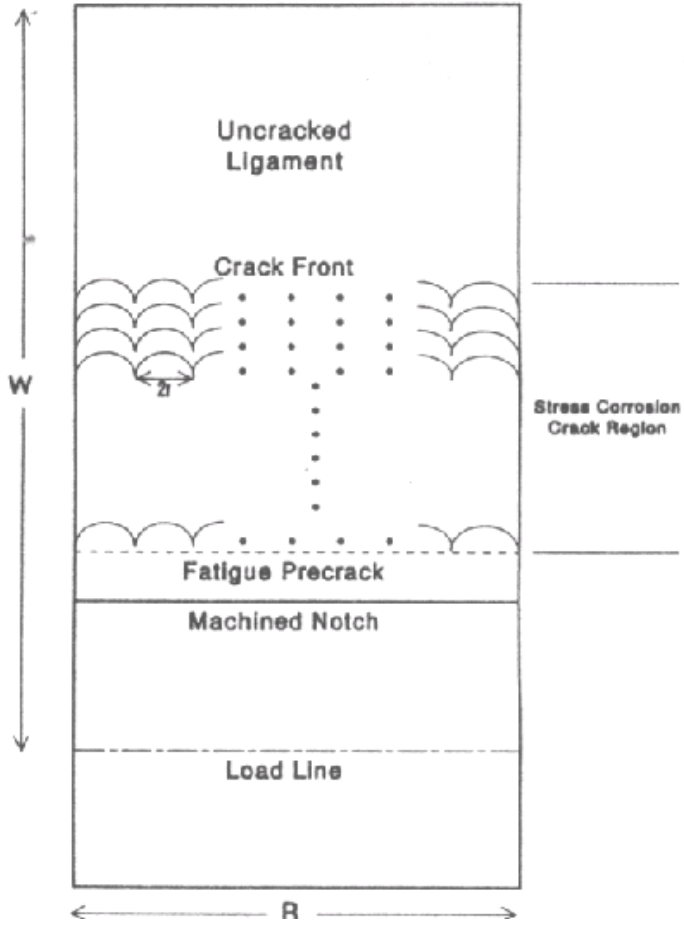

Proposed fracture mechanism, in which the crack advances in a series of brittle, micro fracture events at the crack front.

Brittle Micro Fracture Event Size

$$\frac{da}{dt} = \frac{fr}{B/2r} = \frac{2r^2 f}{B}$$

f **= Frequency of brittle micro fracture event (~ 2 s-1)**

B **= Width of specimen (1.27 cm)**

r **= Radius of brittle micro fracture event ~ 2-3μm.**

Given a grain size of 20 – 50 μm, there should be roughly 4 to 10 events in each package, which is in good agreement with experiment. The remarkable conclusion is that, in this case, the crack advances fracture event-by-fracture event with minimal overlap between events (in this particular case).

Crack Growth Rate Depends on Crack Length

- CEFM predicts that the crack growth rate decreases exponentially with increasing crack length. Also occurs for other localized corrosion phenomena (e.g., pitting).
- Readily understood in terms of the CEFM and the IR potential drop down the crack subtracting from the potential available for driving the processes in the external environment and on the external surface.
- Implies that, eventually, all pits must "die" (repassivate) when the available potential drop is no longer sufficient to drive the processes that occur externally to the crack.
- Must define two crack lengths when discussing SCC and CF; an electrochemical crack length
- Of major significance in predicting the accumulation of damage.

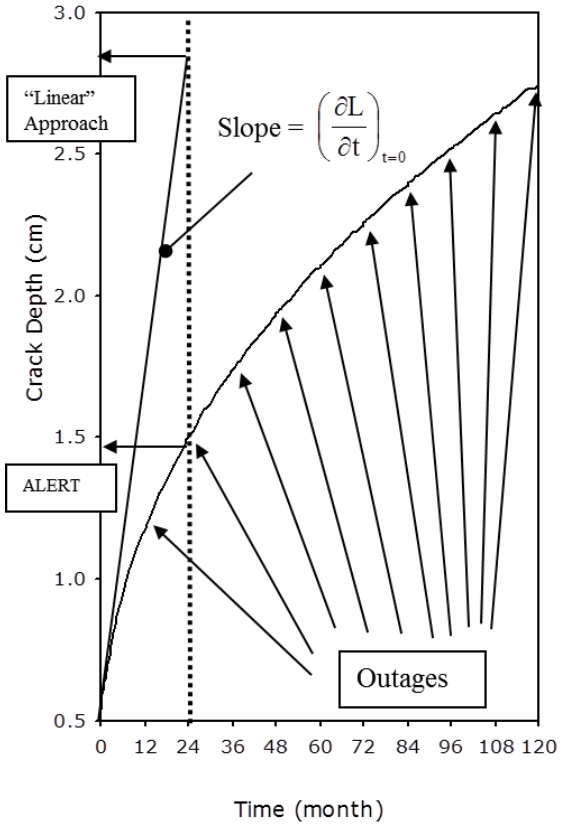

Impact of the dependence of crack growth rate on crack length on the accumulated damage (crack length) for a crack in the inner core shroud surface of a boiling water reactor.

Crack Growth Rate Depends on State of Catalysis of the External Surfaces

- **Theory (CEFM) predicts that the CGR depends sensitively on the extent of catalysis/inhibition of the ORR on the external surfaces, because the kinetics of the ORR determine the magnitude of the coupling current that can be consumed.**
- **Experimental work by T.-K. Yeh in Taiwan suggests that the crack growth rate is higher with Pt-catalyzed surfaces, indicating a relationship between the catalytic properties of the external surface with respect to the oxygen electrode reaction and the crack growth rate.**
- **In the work described here, the coupling current for catalyzed nickel cathodes (500 μA) is considerably higher than that observed with uncatalyzed Type 304 SS cathodes (10 μA). Because a linear relationship between CGR and the coupling current has been found and predicted by the CEFM, this strongly suggests that the CGR is higher under catalytic conditions.**
- **Experimental work from Penn State demonstrates that inhibition of the cathodic reaction (O_2 reduction) on the external surface by the presence of a resistive ZrO2 film causes the crack growth rate to drop to zero, within the accuracy of the experiment. This result is predicted by the CEFM.**

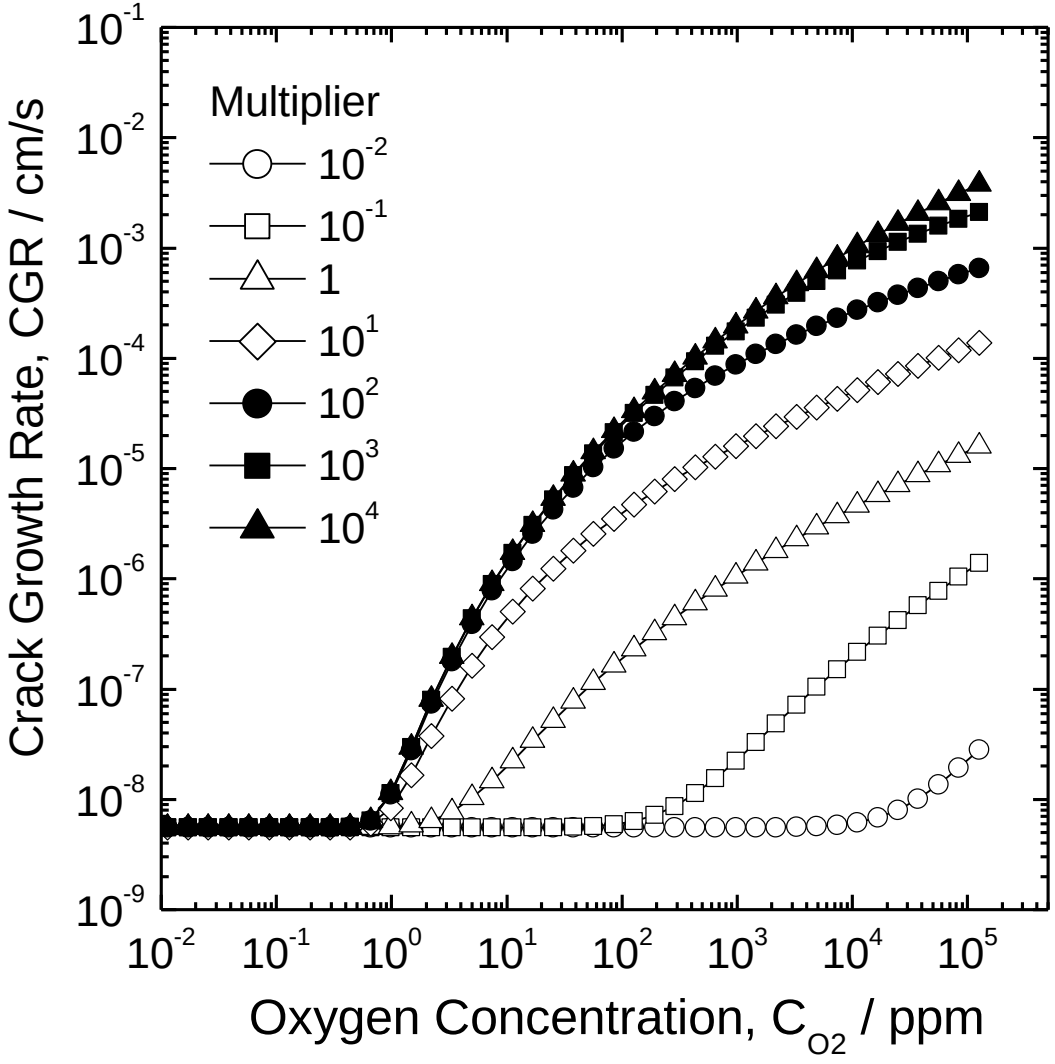

Calculated CGR as a function of [O_2] for AA5083 in 3.6 % NaCl solution at ambient temperature.

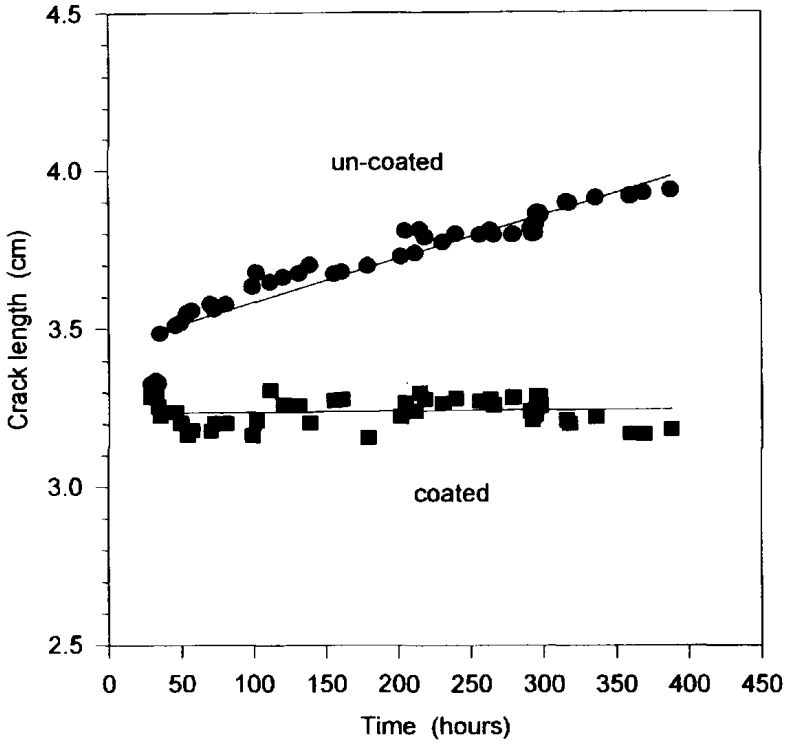

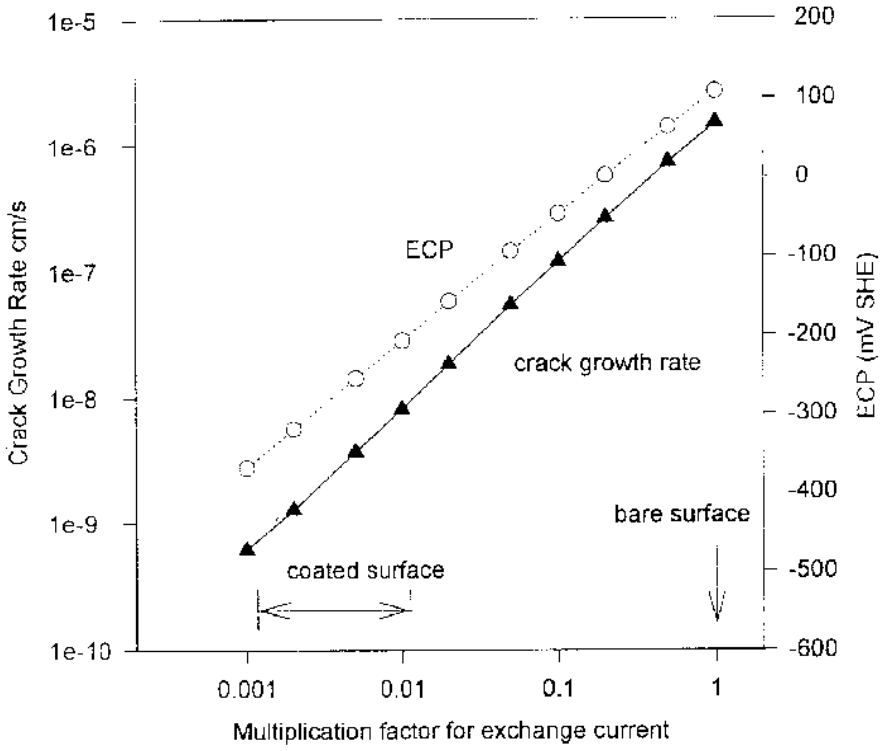

Inhibition of IGSCC in Type 304SS by a dielectric ZrO_2 coating on the specimen external surfaces. The conductivity of the solution was 220 µS/cm at 25 °C and the solution was saturated with O_2 at ambient temperature ($[O_2]$ = 40 ppm). K_I = 25 MPa√m, T = 288 °C. The crack growth rate for the uncoated specimen is 4×10^{-7} cm/s while that for the coated specimen is < 2×10^{-8} cm/s.

Calculated ECP and IGSCC crack growth rate for sensitized Type 304 SS according to the MPM and CEFM, respectively, corresponding to the experimental conditions summarized in Figure 9. Other model parameters are given in Ref. [22].

What Have We Learned Experimentally?

- **IGSCC in sensitized Type 304 SS in simulated BWR primary coolant occurs in discrete steps of 2-3μm dimension.**
- **This dimension is too large to be accounted for by a mechanical slip/dissolution/repassivation process, which should yield a fracture dimension of a few nm, consistent with the Burger's vector of the slip system. Instead, the dimension is consistent with hydrogen-induced cracking (HIC) at the crack tip.**
- **The fracture dimension is relatively independent of the stress intensity factor, but the frequency of fracture follows the dependence of the crack growth rate on stress intensity. This shows that the frequency of fracture is stress (mechanically)-controlled, but the dimension is not.**
- **IGSCC in sensitized Type 304 SS is electrochemical-mechanical in mechanistic character and hence any model developed for predicting crack growth rate must reflect that mixed character. However, what are the separate contributions of electrochemistry and mechanics to the mechanism of IGSCC in sensitized Type 304 SS?**
- **Important independent variables appear to be the stress intensity factor, electrochemical potential, temperature, solution conductivity, degree of sensitization, flow velocity, and pH.**

Artificial Neural Network

An ANN is inspired by the functioning of the brains of living organisms comprising billions of neurons of the type depicted below with all being connected within a processing network.

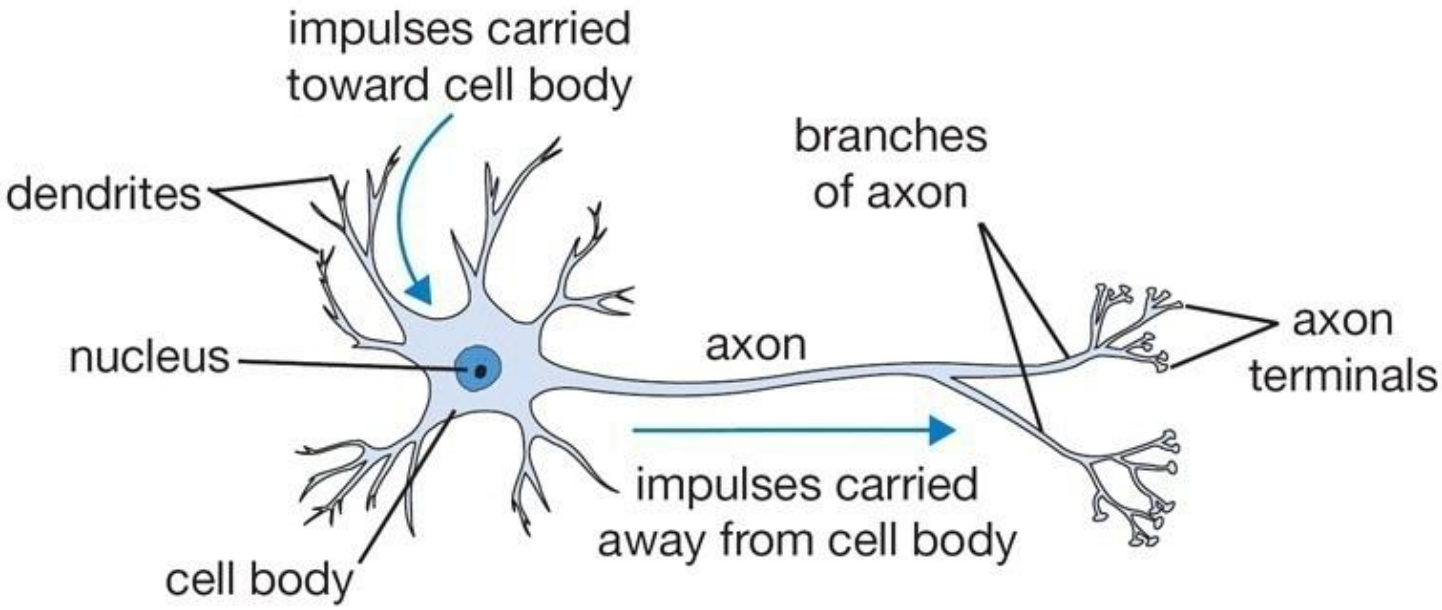

http://www.wpclipart.com/medical/anatomy/cells/neuron/

Architecture for ANN

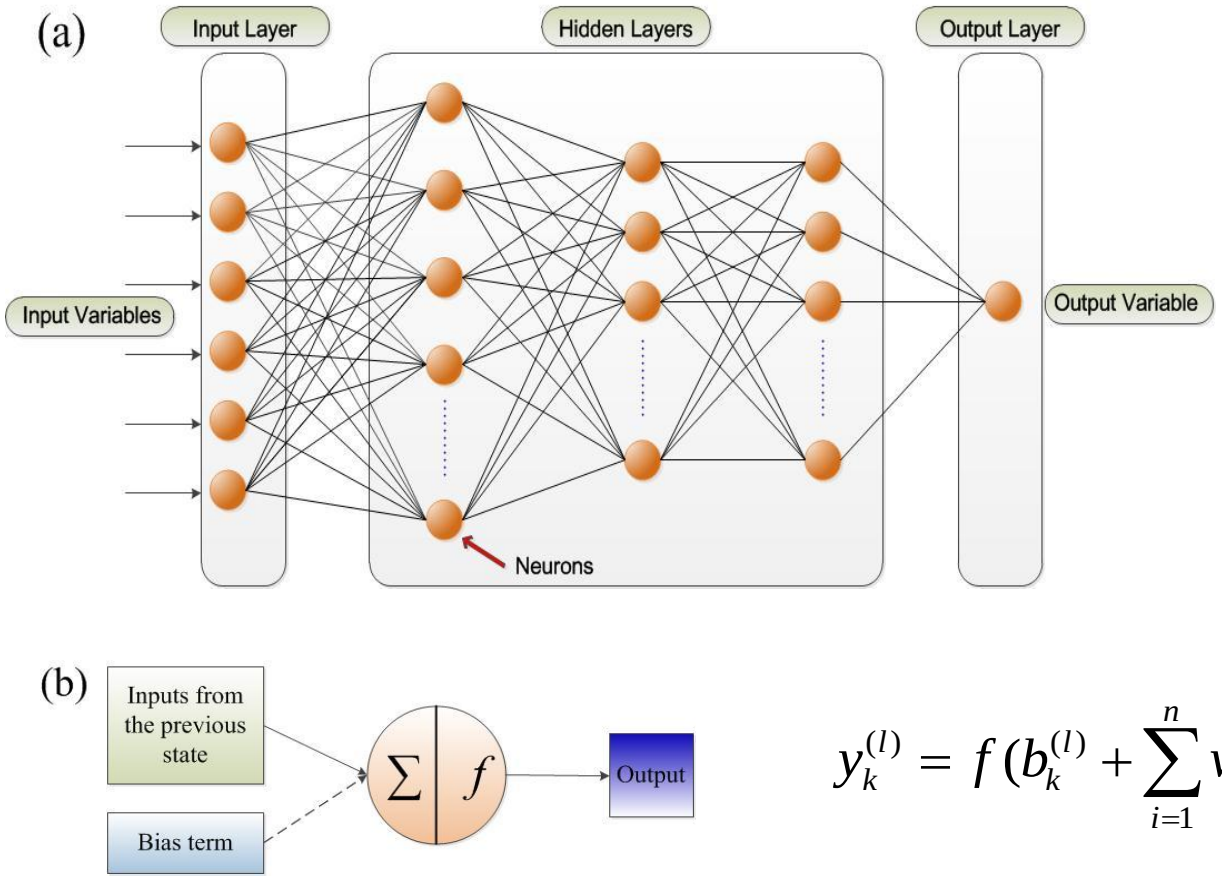

Figure 1: (a) The topology of the artificial neural networks (ANN) used in this work (b) schematic of each neuron in the network. Σ signifies summation, while *f* represents the transformation (sigmoid function).

Data preprocessing and partitioning

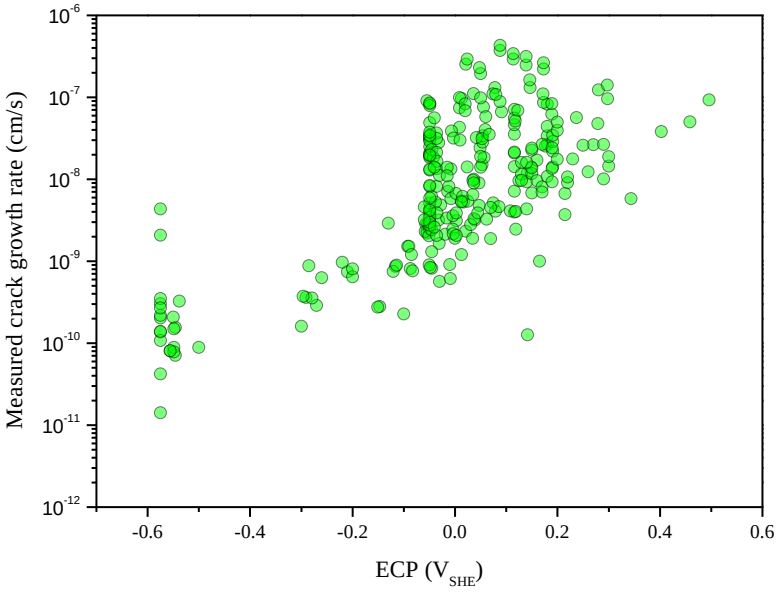

Crack growth rate vs. corrosion potential for Type 304 stainless steel.

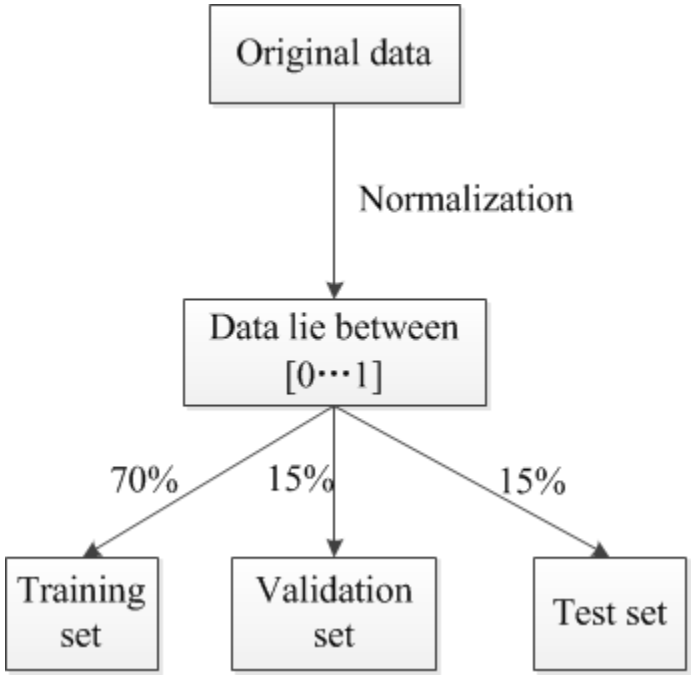

ANN training performance

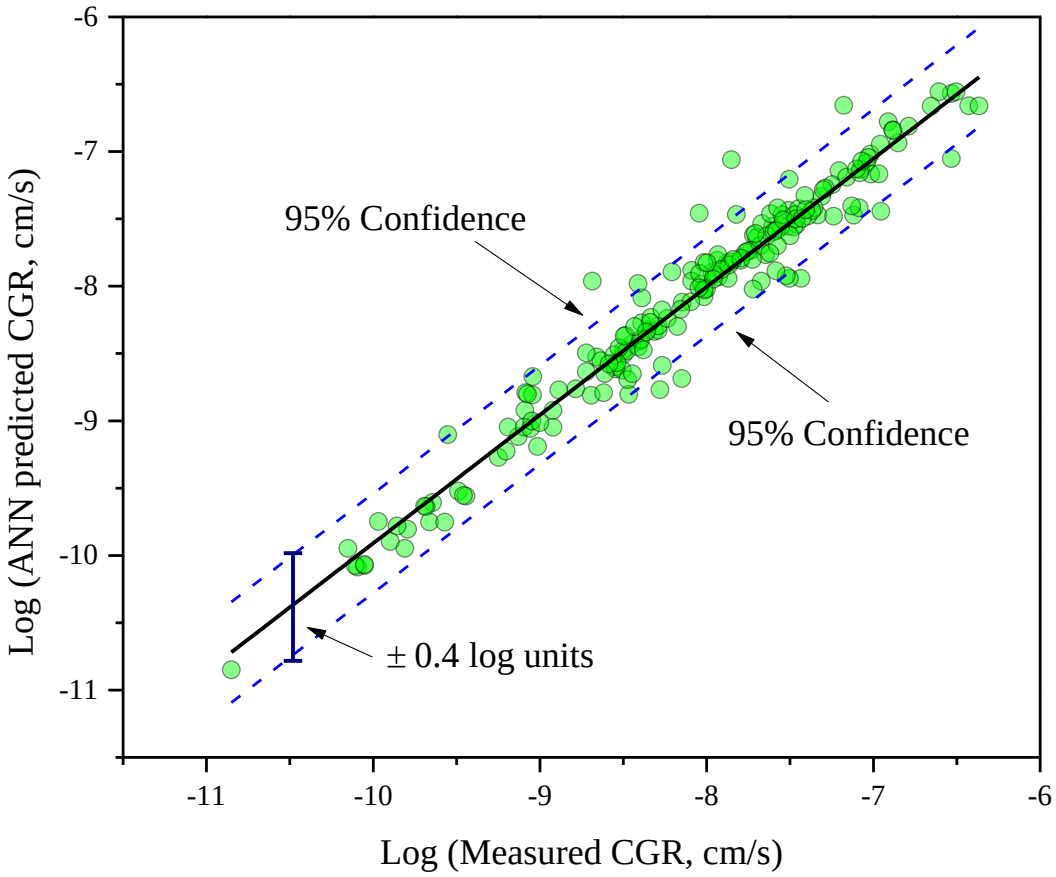

Comparison of predicted values vs. experimental data after training of the ANN.

Coupled Environment Fracture Model

- **Originally developed in early 1990s (Macdonald and Urquidi-Macdonald) to predict crack growth rate in sensitized Type 304 SS in BWR primary coolant circuits. Since expanded to other systems.**
- **Proven to be highly effective at predicting CGR even when calibrated on only two datum at different temperatures.**
- **Provides a good case study for the development of a deterministic model, since the model has undergone a number of iterations.**
- **Model has been extensively tested and is included in several codes for predicting the accumulation of stress corrosion cracking damage in BWR primary coolant circuits.**
- **Extended to fatigue loading (this conference) and to hydrogen-induced cracking (HIC).**

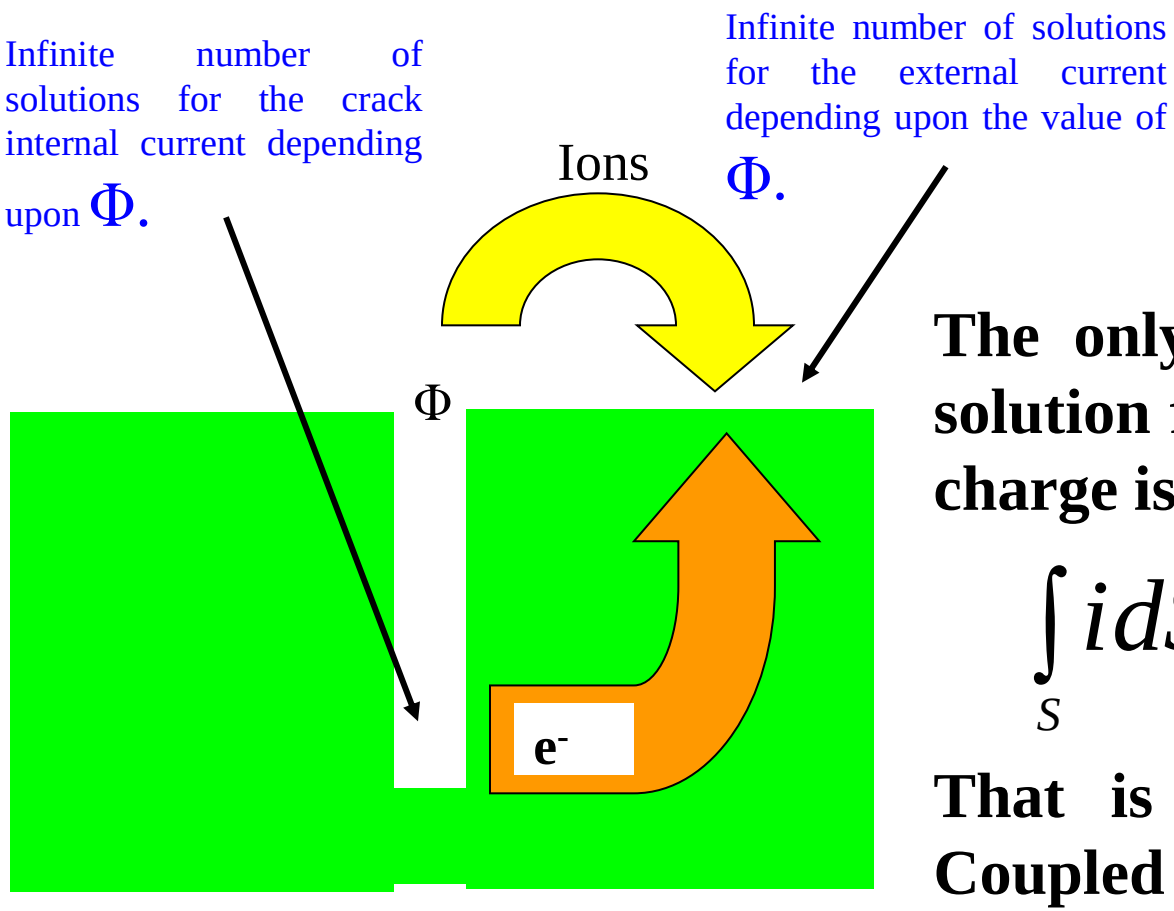

The only physically viable solution for Φ is that which charge is conserved.

$$\int_S i dS = 0$$

That is the basis of the Coupled Environment Fracture Model (CEFM).

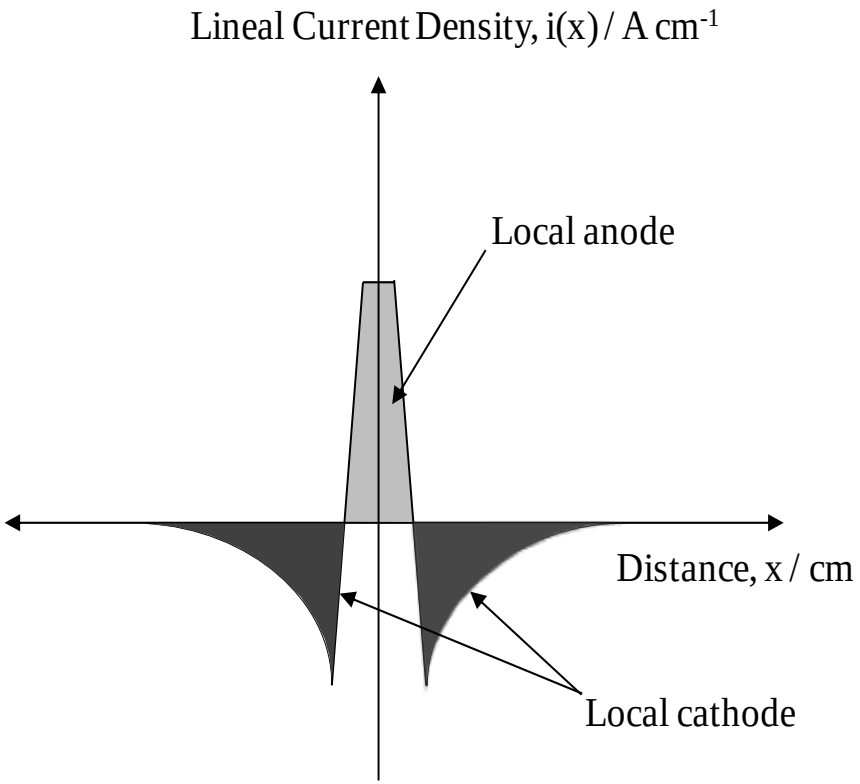

Schematic of the current distribution in a growing crack. The conservation of charge requires that the area of the region over which anodic processes dominate (grey region) and the region over which cathodic processes dominate (black region) must be equal and sum to zero. This condition establishes the potential at the cavity mouth, while electro-neutrality establishes the potential at the cavity tip. The potential on the external surface remote from the mouth is given by $-E_{corr}$ where E_{corr} is the corrosion potential. All potentials are electrostatic potentials in the solution with respect to the metal or with respect to a chosen reference electrode.

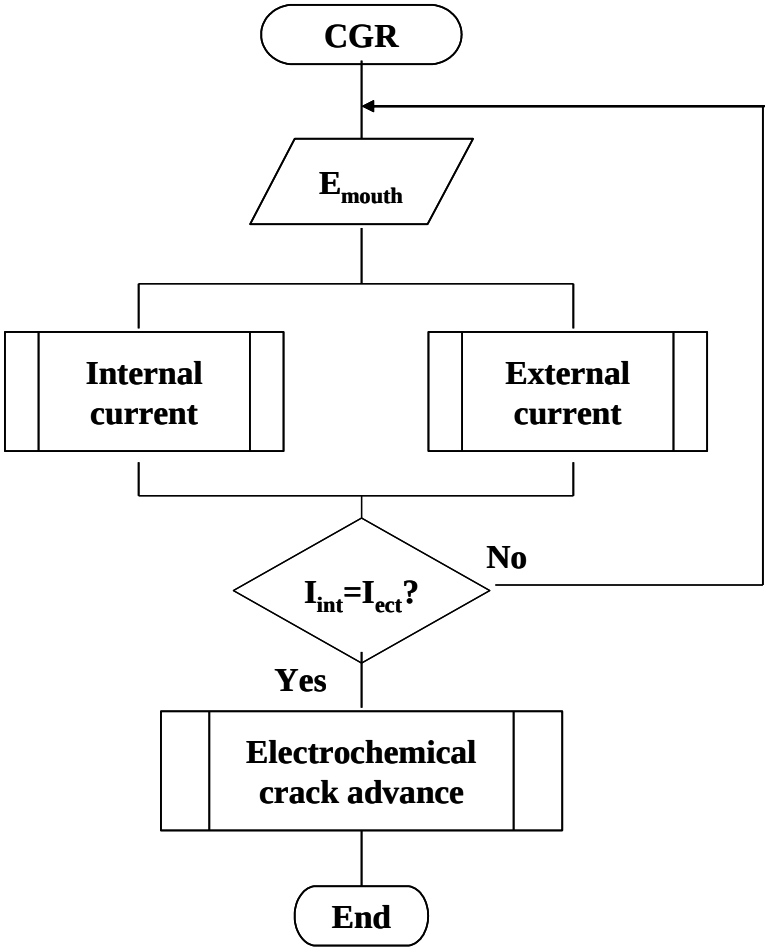

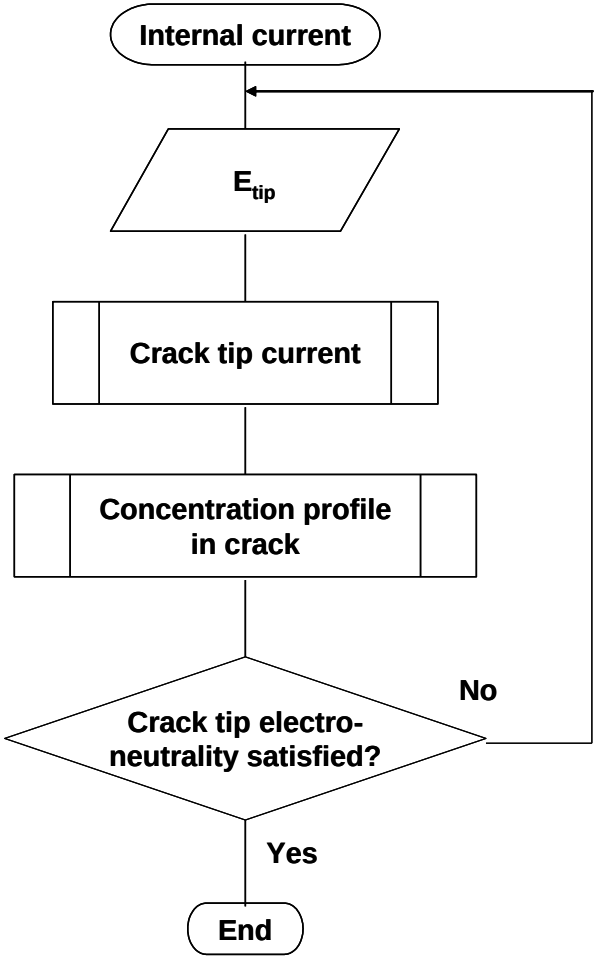

Charge conservation - Iteration on the mouth potential, E_{mouth}.

Electroneutrality – Iteration on the crack tip potential, E_{tip}.

Coupled environment fracture model

Table 1 Values for parameters in the CEFM for Type 304 stainless steel

Parameter	Value	Source
Atomic volume (m^3)	1.18×10^{-29}	[6]
Fracture strain of oxide film, ε_f	8×10^{-4}	[1]
Young's modulus, E(MPa)	2×10^{5}	[6]
Dimensionless constant, β	5.08	[67]
Density, ρ(g/cm^3)	8	[6]
Yield strength, σ_y(MPa)	215	[67]
Strain hardening exponent, n	1.7	[67]
Dimensionless constant, λ	0.11	[67]
Shear modulus, G(Pa)	7.31×10^{10}	[6]
Grain-boundary self-diffusion coefficient, D_{b0}(m^2/s)	2.50×10^{-4}	[68]
Activation energy for diffusion (kJ/mol)	168	[68]
Grain-boundary diffusion width (m)	5×10^{-10}	[68]
Tafel slope for HER	0.065	[5]
i_0 for HER (A/cm^2)	5×10^{-4}	[5]
Tafel slope for ORR	0.071	[5]
i_0 for ORR (A/cm^2)	5.05×10^{-3}	[5]
Passive current density at steady state (A/cm^2)	2.6×10^{-3}	[5]
Standard electrochemical potential for stainless steel dissolution reaction, E_0(V_{SHE})	-0.47	[69]

Crack tip strain rate: $$\frac{d\varepsilon_{ct}}{dt}=\beta\left(\frac{\sigma_y}{E}\right)\left(\frac{n_{GH}}{n_{GH}-1}\right)\left\{\ln\left[\left(\frac{\lambda}{n}\right)\left(\frac{K}{\sigma_y}\right)^2\right]\right\}^{\frac{1}{n_{GH}-1}}\left[\left(\frac{2}{K}\right)\dot{K}+\frac{\dot{a}}{r}\right]$$

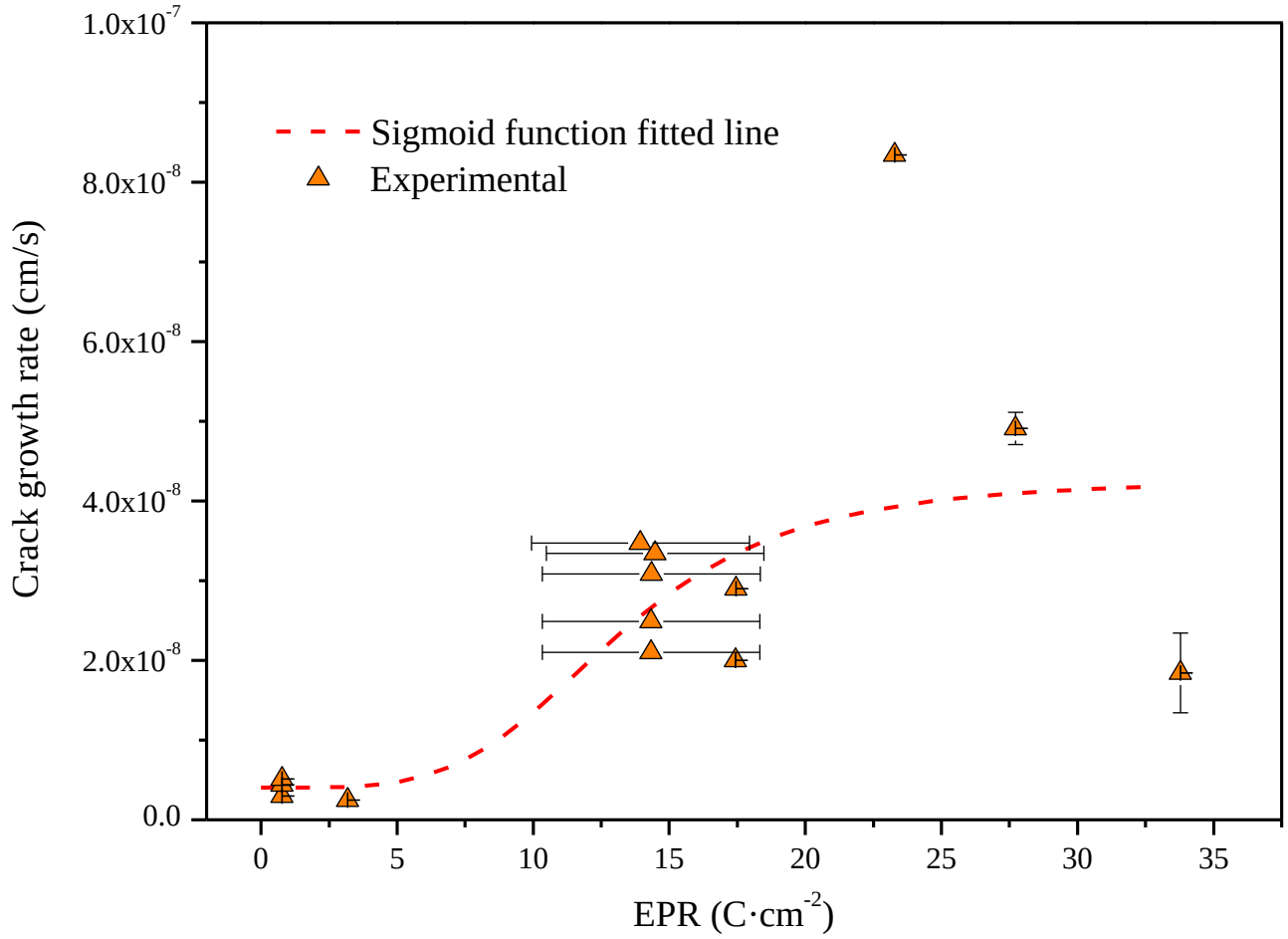

Simulated dependence of CGR on DoS using a sigmoid function.

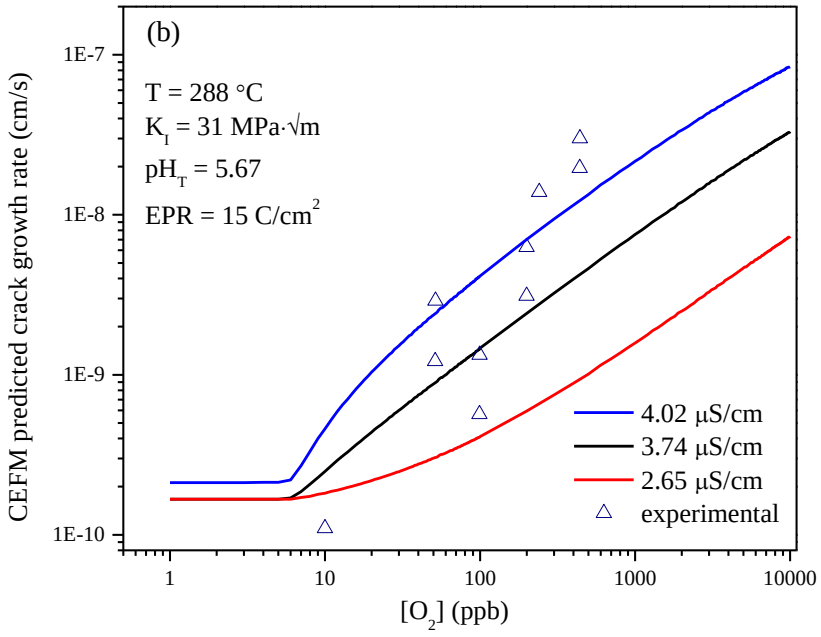

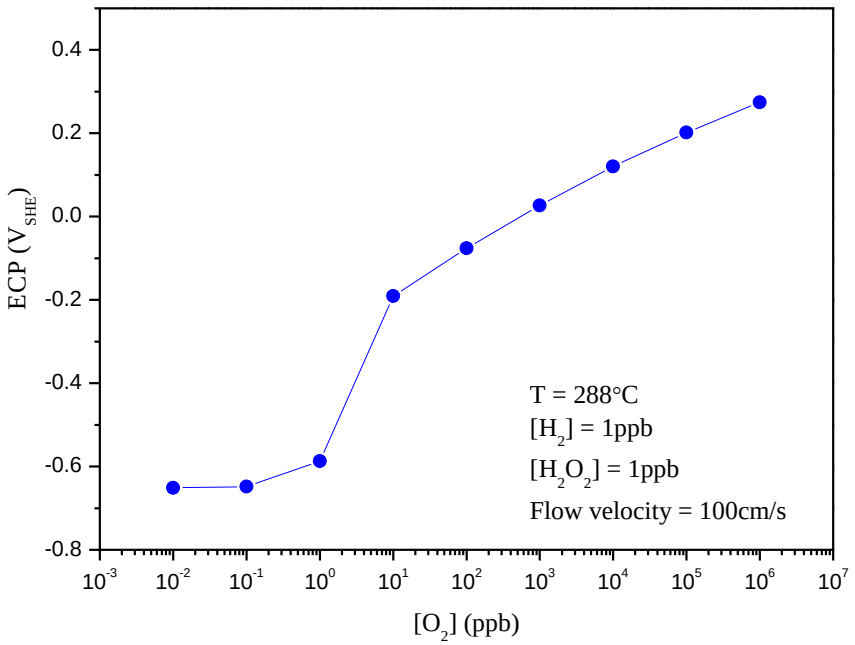

Dependence of CGR on $[O_2]$ at different conductivities, as predicted using the ANN (a) and the CEFM (b). Parameter values used in the CEFM are given in Table 2.

Dependence of ECP on $[O_2]$ at 288°C, as calculated by the MPM.

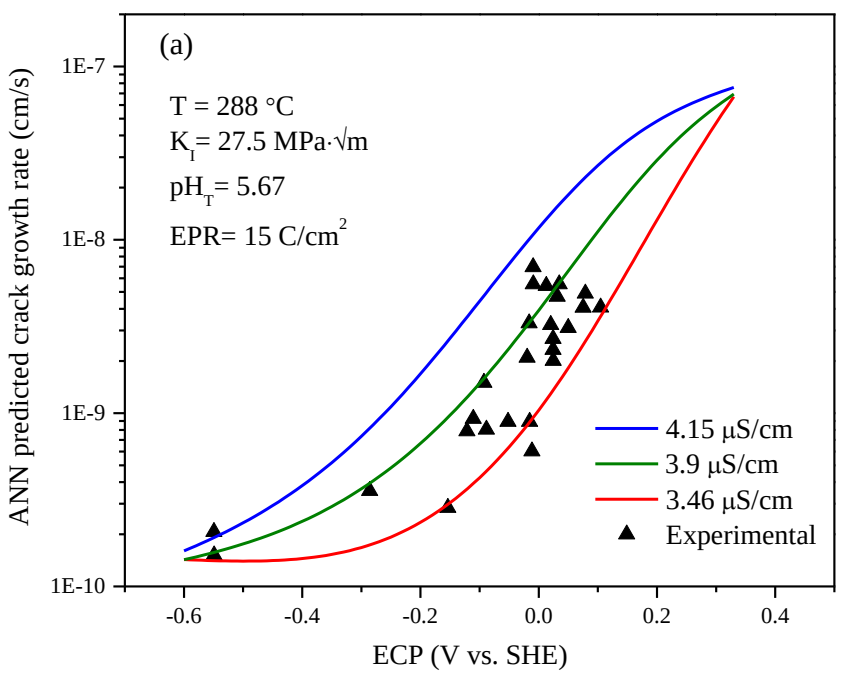

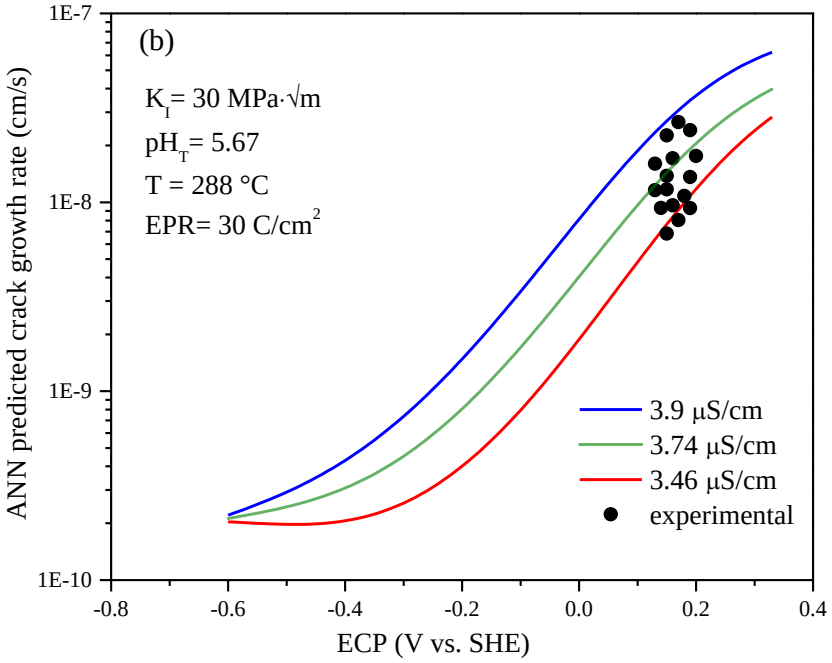

Dependence of CGR on ECP as predicted using the ANN for different values of the stress intensity factor (K_I) and degree of sensitization (DoS). Experimental data come from * ** with conductivity values lying between 0.06µS/cm and 0.4µS/cm at ambient temperature. The conductivities shown in the figure correspond to those calculated for 288ºC.

*** P.L.Andresen, Corrosion, 47(1991)917-938**

****Stress Corrosion Crack Growth Rate Measurements on Unsensitized Type 304 Stainless Steel in 288ºC Water, EPRI, Palo Alto, CA, TR-113489 (2000).**

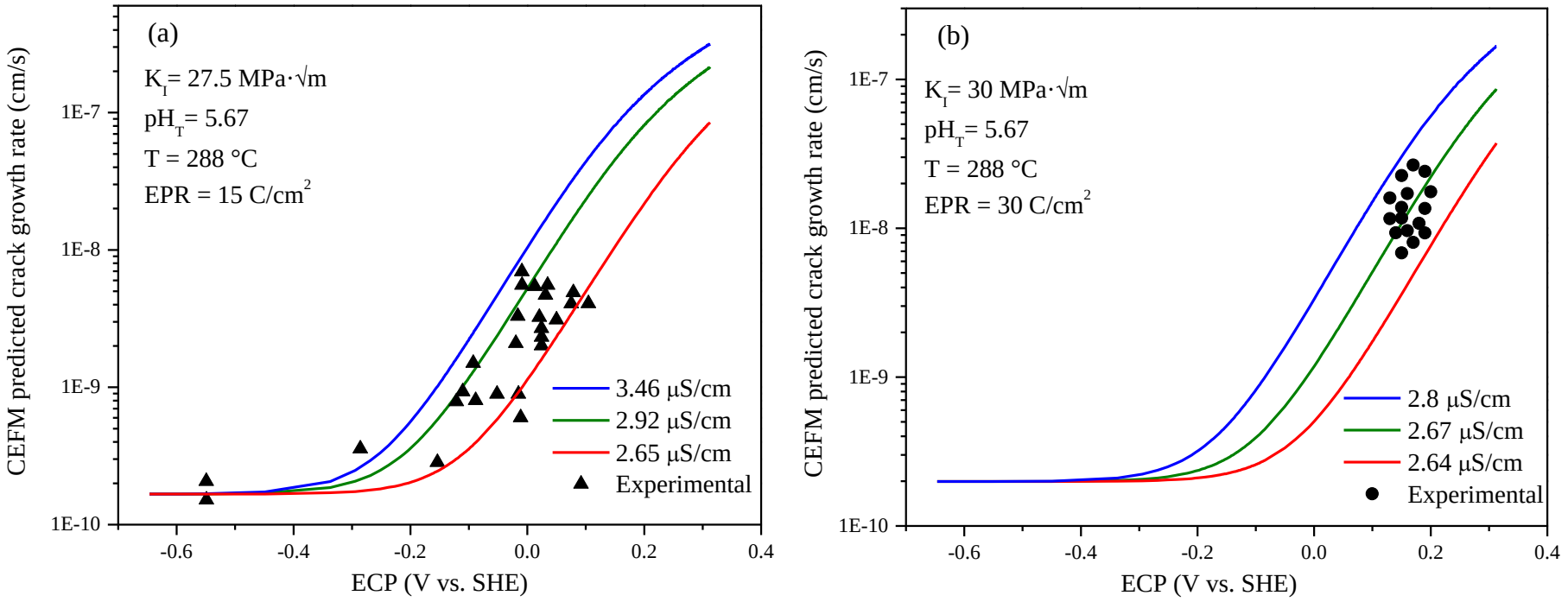

Dependence of CGR on ECP as predicted for different values of the stress intensity factor (K_I) and the degree of sensitization (DoS) using the CEFM. Model parameters are as given in Table 2. Experimental data come from [20] [41] with conductivity values lying between 0.06µS/cm and 0.4µS/cm at ambient temperature. The conductivities shown in the figure correspond to those calculated for 288°C.

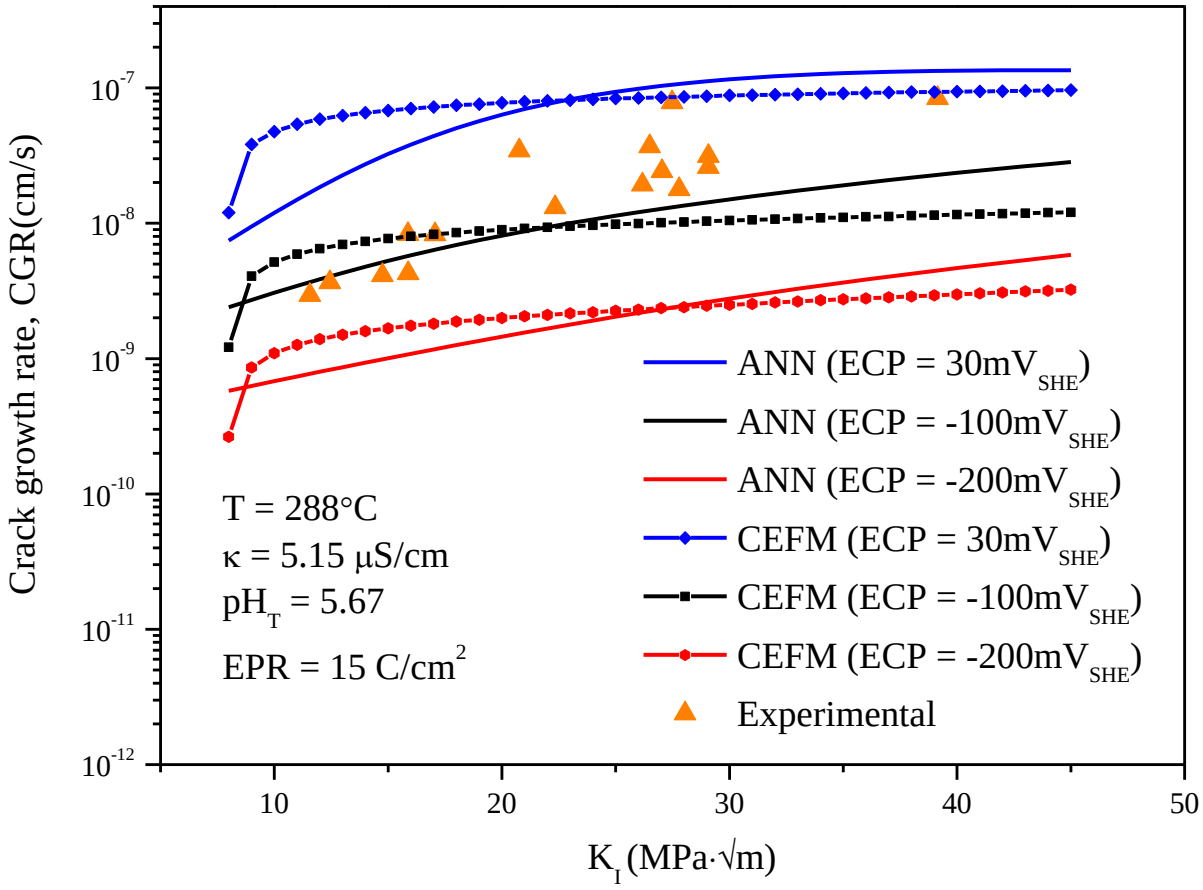

Comparison of the dependencies of CGR on stress intensity factor (K_I) for different values of the ECP, as predicted by the ANN and the CEFM. The parameter values used in the CEFM are given in Table 2.

Degree of Sensitization

- **Historically, the degree of sensitization (DoS), which measures the extent of chromium depletion due to chromium carbide precipitation (Cr23C7) on the grain boundaries as measured by reverse polarization reactivation, has always bee recognized as an important parameter in controlling IGSCC crack growth rate in sensitized stainless steels and in nickel-based alloys.**
- **Our analysis suggests that the impact of DoS on CGR can be represented by the following function:**

$$CGR_{calibrated} = CGR \times \left(1.5047 - \frac{1.3627}{1 + \left(\frac{DoS}{13.17753}\right)^{4.09718}}\right)$$

where $CGR_{calibrated}$ and CGR are the crack growth rate for any value of DoS and the crack growth rate of sensitized 304SS for DoS values of 15 C/cm^2, respectively.

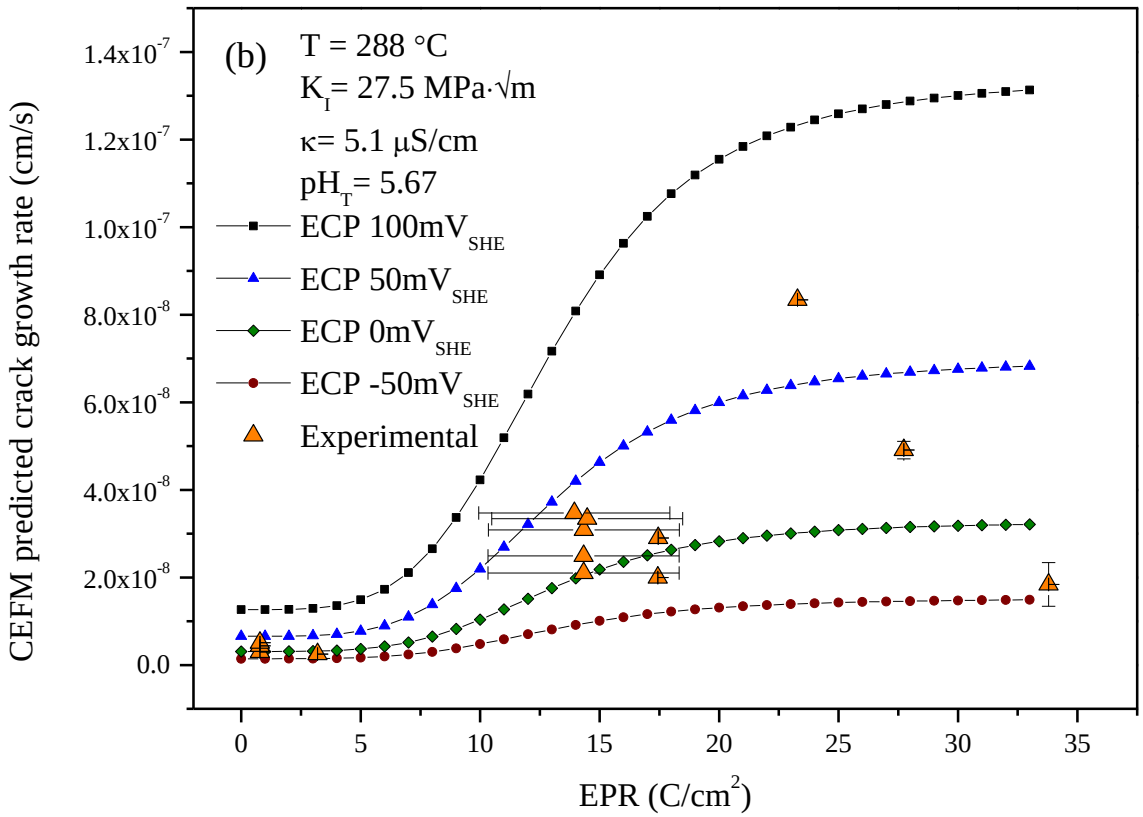

Dependence of CGR on degree of sensitization (DoS) as a function of ECP, as predicted using the ANN (a) and the CEFM (b). Parameter values used in the CEFM are given in Table 2.

Sensitivity analysis

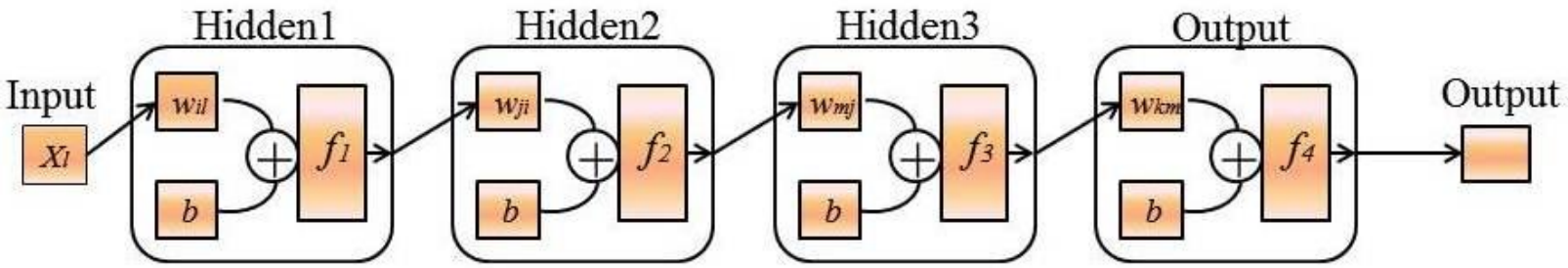

Pad (partial derivatives) method

$$S_{k,l}^{p} = \frac{\partial o_k}{\partial x_l} = o_k^{'} \sum_{m=1}^{M} (w_{km} d_m^{'} \sum_{j=1}^{J} w_{mj} z_j^{'} \sum_{i=1}^{I} (w_{ji} y_i^{'} w_{il}))$$

$$SSD_i = \sum_{p} (\frac{\partial o_k^p}{\partial x_l^p})^2$$

Contribution of i_{th} variable= $\dfrac{SSD_i}{\sum_i SSD_i}$

The breadth of the database is such that only the impact of temperature, ECP, stress intensity, conductivity, and degree of sensitization could be included in the analysis.

Table 1 Relative importance of input variables on the value of crack growth rate

Input variable	Range	Importance (%)
Stress intensity ($MPa \bullet m^{0.5}$)	10.4-67.7	17
Temperature (℃)	25-292	25.4
Conductivity (μs/cm)	0.52-5.72	24.3
Electrochemical potential (V_{SHE})	-0.575 to +0.496	18.9
Degree of sensitization (C/cm^2)	0-33.79	14.4

- IGSCC in sensitized Type 304SS in BWR primary coolant is primarily an electrochemical process with significant mechanical character.

Summary and Conclusions

The principal findings of this study are as follows:

- **Based on experimental data and calculation, where it was needed to estimate missing independent parameter values (T, ECP, κ, K_I, pH, and DoS), a comprehensive data base for the training of an artificial neural network (ANN) for IGSCC in sensitized Type 304 SS in simulated BWR primary coolant environments (water at 288^{o}C) was developed. The data employed had been obtained using pre-cracked C(T) fracture mechanics specimens, with which the crack growth rate, free of crack initiation issues, was reported by various authors. The ANN was trained on 70 % of the database using back propagation error minimization in the "pattern recognition" mode, while 15% of the data were used as the validation set and the remaining 15% were used as the test set. In this manner, an effective ANN for predicting IGSCC crack growth rate in sensitized Type 304SS was devised.**
- **The predicted CGRs obtained from the trained ANN are in good agreement with the experimental data that were used for evaluation purposes. This comparison indicates that the uncertainty in the measured crack growth rate data available in the literature/database is of the order of ± 0.4 log units. Much of this uncertainty arises from the failure of many experimenters to measure important independent variables, such as the corrosion potential (ECP), high temperature conductivity, pH, and flow velocity (mass transport rate).**
- **Sensitivity analyses of the ANN ascertained the contributions of the various independent variables to determining the crack growth rate, indicated that temperature and conductivity are the two of the most important impact factors in determining CGR, followed by electrochemical potential, stress intensity factor, and degree of sensitization. This sensitivity analysis establishes that IGSCC in sensitized Type 304SS in high temperature aqueous environments is primarily an electrochemical process with significant mechanical character.**
- **The coupled-environment fracture model (CEFM) has been extended to take into account the degree of sensitization of the steel, by incorporating an empirical sigmoid functional dependence of CGR on DoS, as established by the ANN. The extended CEFM has been used to predict crack growth rate as a function of the various independent variables, and through a comparison with the dependent variable/independent variable relationships uncovered by the ANN, it is apparent that the CEFM provides high fidelity prediction of the IGSCC crack growth rate within the error limits of the experimental data, in sensitized Type 304SS in BWR primary coolant environments.**

Acknowledgements

The authors gratefully acknowledges the financial support from National Key Basic Research Program of China (No.2011CB610505 and 2014CB046801), Specialized Research Fund for the Doctoral Program of Higher Education (20120032110029). JS also appreciates the support of the China Scholarship Council for supporting his study abroad.